# Ultrasound elicits behavioral responses through mechanical effects on neurons and ion channels in a simple nervous system

**Jan Kubanek[1], Poojan Shukla[1], Alakananda Das[1], Stephen Baccus[2], Miriam B. Goodman[1]**

[1]Department of Molecular and Cellular Physiology, 279 Campus Drive, Stanford, CA 94305

[2]Department of Neurobiology, 291 Campus Drive, Stanford, CA 94305

## Abstract

Focused ultrasound (US) can stimulate specific regions of the brain non-invasively in animals and humans. This new brain stimulation method has the potential to provide a spatially precise treatment of neurological disorders and to advance brain mapping. To realize this potential, it is crucial to discover how US stimulates neurons. Toward this end, we devised a genetic dissection assay leveraging the well-characterized nervous system of *C. elegans* nematodes. We found that focused US (0.6–1.0 MPa, 10 MHz) elicits robust reversal behavior in wild-type animals. The response is preserved in animals deficient in thermosensation, yet absent in animals lacking neurons responsible for low-threshold touch sensation. We further found that the mechanical response rests on a properly functioning DEG/ENaC ion channel. Deletion of its MEC-4 subunit abolishes the response. The evidence for a mechanical nature of the response allowed us to maximize mechanical stimulation by pulsing the stimulus at specific pulse repetition frequencies (PRFs). The optimal range of PRFs aligned with that used for US neuromodulation in large mammals including humans, and is consistent with the prediction of a recent molecular model of mechanosensation. Thus, the mechanical forces associated with US are capable of activating mechanosensitive ion channels in a freely behaving animal. The mechanical nature of the effect proposes a specific pulsing protocol to activate neurons that possess mechanosensitive properties in the peripheral and central nervous systems of animals and humans.

## Introduction

Low-intensity focused ultrasound (US) stimulates neurons in animals and humans (Harvey, 1929; Fry and others, 1958; Meyers et al., 1959; Foster and Wiederhold, 1978; Gavrilov et al., 1996; Tufail et al., 2011; Yoo et al., 2011; Deffieux et al., 2013; Menz et al., 2013; King et al., 2013; Legon et al., 2014; Lee et al., 2015; Lee et al., 2016; Lee et al., 2016) and is emerging as a noninvasive way to stimulate specific regions in the brain. In comparison to transcranial magnetic stimulation (TMS), US can propagate deep into the brain while also retaining relatively sharp spatial focus (1–5 mm, depending on the frequency used

to penetrate skull of a particular thickness). As such, US has the potential to provide a spatially focused and depth-penetrating alternative to TMS.

It is currently unknown how US stimulates neurons and what stimulus protocol delivers optimal stimulation. This knowledge gap presents a significant barrier to utilizing US for non-invasive neural stimulation. There have been several candidate mechanisms considered. The effect may be due to heating, which affects many physiological processes. However, only small temperature increases (on the order of 0.1°C) have been computed and measured during US applications for neuromodulation (Tufail et al., 2010; Yoo et al., 2011; Menz et al., 2013). Alternatively, propagating US may exert mechanical effects in the target tissue, of several possible forms. First, US may elicit cavitation, a phenomenon characterized by formation and collapse of gaseous bodies in liquid media or soft tissues. The bubble-mediated effects of US can have mechanical, thermal, and destructive effects on biological tissues (Ibsen et al., 2015). Nonetheless, physiological effects of US have been observed without microbubbles and at frequencies and intensities that are unlikely to produce cavitation (Menz et al., 2013). Second, US may affect lipid bilayer dynamics and so alter membrane capacitance according to modeling work (Krasovitski et al., 2011; Plaksin et al., 2014). This work has not, thus far, found robust experimental support (Rohr and Rooney, 1978; Prieto et al., 2013). Other mechanical effects on cellular membranes have been proposed (Tyler, 2011). Third, it has been hypothesized that the mechanical forces associated with US may affect the activity or conformation state of ion channels or other molecules sensitive to membrane stretch (Tyler et al., 2008; Tyler, 2012; Kubanek et al., 2016).

To provide further insights into ultrasound neurostimulation, we devised a behavioral-genetic assay based on the nematode *C. elegans* that leverages the extraordinary sensitivity of this animal to both mechanical and thermal stimuli, its simple behavioral repertoire, and well-characterized tools for genetic dissection. The animal can detect thermal fluctuations as small as 0.05°C (Ramot et al., 2008) and forces as low as 50 nN (O'Hagan et al., 2005). We recorded and quantified the ability of US to evoke reversals in wild-type animals and compared the responses with mutants defective in specific sensations, neurons, and ion channels.

# Materials and Methods

## Animals and strains

The *C. elegans* nematodes used in this study were cultivated and age-synchronized by hypochlorite treatment (Stiernagle, 2006) at 15 or 20°C. Neither cultivation temperature nor ambient temperature

and humidity of the experimental room had a detectable effect on behavioral response frequency (data not shown).

The following strains were analyzed: N2 (Bristol); CB1338 *mec-3(e1338)* IV; CB1611 *mec-4(e1611)* X; TU253 *mec-4(u253)* X; IK597 *gcy-23(nj37)gcy-8(oy44)gcy-18(nj38)*) IV; VC1141 *trp-4(ok1605)* I; VC818 *trp-4(gk341)* I; TQ296 *trp-4(sy695)* I; GN716 *trp-4(ok1605)* I, outcrossed four times from VC1141. All mutants are derived from the N2 (Bristol) background, which serves as the wild-type strain in this study. All strains were obtained either from a repository maintained in the Goodman lab or from the Caenorhabditis Genetics Center.

The allele *mec-3(e1338)* is a null allele of the *mec-3* gene needed for proper cell-fate determination of ten mechanoreceptor neurons: the six TRNs, two FLPs, and two PVD neurons (Way and Chalfie, 1989). *mec-4(e1611)* and *mec-4(u253)* represent gain-of-function and null alleles of the *mec-4* gene encoding the key pore-forming subunit of native mechano-electrical transduction chanels in the TRNs, respectively (Schafer, 2015). *mec-4(e1611)* mutants lack TRNs due to degeneration caused by unregulated channel activity (Driscoll and Chalfie, 1991). All *mec-3* and *mec-4* mutants are strongly touch-defective in classical touch assays. The *gyc-8gcy-18gcy-23* triple mutants lack a trio of receptor guanylate cyclases expressed exclusively in the AFD thermoreceptor neurons and are insensitive to thermal gradients (15-25°C) and defective in thermotaxis (Garrity et al., 2010; Glauser and Goodman, 2016).

The *trp-4(ok1605)* allele contains a 1kb deletion encompassing exons 12-14. The loss of these exons predicts an in-frame deletion in the region of the transcript coding for ankyrin repeats 16-21. The *trp-4(gk341)* allele contains a small deletion encompassing exon 2. The loss of this early exon predicts a frame-shift in the transcript leading to an early stop in translation. The *trp-4(sy695)* allele contains an unmapped 3kb deletion in the 3' region of the gene. This deletion predicts a disruption in the transmembrane ion-channel domain. The *trp-4(ok1605)* outcross was performed four times with wildtypes (N2).

## Imaging and transducer control

For each assay, we transferred a single adult animal from a growth plate to a 4 mm-thick NGM agar slab that was free of bacteria. To create a boundary sufficient to retain the animal within the camera's field of view, we used a filter paper ring saturated by a copper sulfate (500 mM) solution.

A commercially-available piezoelectric ultrasonic transducer (A327S-SU-CF1.00IN-PTF, Olympus, 1-inch line-focused) was positioned 1 inch (2.54 cm) below the top of the agar slab. The axis of the transducer was perpendicular to the slab. The interface between the face of the transducer and the agar slab was filled with degassed water, contained within a plastic cone mounted on the transducer. The

water was degassed by being boiled for 30 min and stored in air-tight tubes. The US transducer had its wavefront focused on a line. Hydrophone measurements did not detect appreciable attenuation of the US pressure amplitude through the pad. The agar slab was illuminated using a circular (20 cm in diameter) array of infrared LEDs. This provided the intensity contrast needed to track animal movement using the Parallel Worm Tracker (Ramot et al., 2008). The contrast was optimal when the plane of the LED array was about 1 cm above the top of the agar slab. We also used a blue LED, controlled by an Arduino Uno board and mounted 5 cm above the agar slab, to deliver an optical signal indicating the stimulus onset.

The signal to drive the US transducer was generated using a HP 8116A (Hewlett-Packard) function generator and modulated to achieve a specific pulse repetition frequency and duration through the Arduino Uno board. The resulting signal was amplified using an ENI-240L amplifier (ENI, Rochester, NY). The output pressures were measured in free field using a calibrated hydrophone (HGL-0200, Onda, Sunnyvale, CA) combined with a pre-amplifier (AG-2020, Onda). The hydrophone measurements were performed at the peak spatial pressure. The hydrophone manufacturer's calibration values around the frequency of 10 MHz were steady and showed only minimal level of noise.

## Behavioral recordings

Freely moving animals were monitored by the video camera in live mode until they approached the ultrasound focus head first and each animal was tested in ten trials with an inter-trial interval of at least 20 s. We initiated video recordings about 5 s before the predicted approach of the focus and kept recording for about 10 s following the delivery of each stimulus. All animals were assayed blind to genotype and as adults. Tested pressure amplitudes were: 0 (sham), 0.2, 0.4, 0.6, 0.8, and 1.0 MPa. This stimulus sequence was repeated 10 times in each animal. The protocol for testing the effects of stimulus duration, duty cycle, and pulse repetition frequency was analogous with the exception that instead of varying pressure levels, we varied the levels of the respective quantities in steps indicated by the respective figures. The 1.0 MPa pressure is the limit of long-term operation that does not cause damage to the transducer.

Each animal's movement was recorded at 20 frames per second at a resolution of 576 x 592 pixels using a digital camera (SME-B050-U, Mightex). We recorded 350 frames per video. The resolution and frame-rate were chosen to be high enough to provide reliable movement characterization while maintaining acceptable size of the stored videos. The image was magnified 3x using a Navitar lens mounted below the camera. The camera's chip spanned 5.6 x 4.2 mm. A previously reported software (Ramot et al., 2008) monitored each animal's centroid and quantified the instantaneous movement direction.

### Quantification of response frequency and baseline response frequency

To determine trials in which US evoked a significant reversal, we computed the average velocity vector during the interval from 250 ms to 1 s following the US onset, and compared it to the average velocity vector during a 1 s period immediately preceding the US onset. We then computed the vector difference, and evaluated the magnitude of that difference. We asked whether this metric was significant with regard to the null distribution of this metric constructed over all baselines (same time windows, just shifted 1 s back in time so that there could be no effect of US) available for a given animal. If a metric value was distant enough from the null distribution such that the probability of it being drawn for the null distribution was less than 0.01, we took the response as significant. We computed the proportion of significant responses over the 10 stimulus repetitions for each animal and refer to this metric as the response frequency.

The computation of the baseline response frequency (dashed lines in the plots) was analogous to the computation of the response frequency with the exception that the metrics were taken in time windows before the US could have any impact (i.e., before the US was turned on). In particular, the velocity difference was computed by comparing a 1 s time window immediately preceding the US to a 1 s time window preceding the US onset by 1 s. The baseline distribution used the same time windows, just shifted back in time by 1 s. The baseline response frequency was indistinguishable across the tested animal strains ($F_{4,95} = 0.28$, $p = 0.90$, one-way ANOVA), and was indistiguishable also across the *trp-4* strains ($F_{3,36} = 0.27$, $p = 0.84$, one-way ANOVA).

### Model of response frequency as a function of duty cycle

To generate the modeled prediction curve in Fig. 6B, the envelope of signals of the specific duty cycle were converted into frequency domain and convolved with the mechanotransduction filter provided by Eastwood et al. (Eastwood et al., 2015). The effective (rms) value of the resulting signal was taken as the model's output. Thus, the model has no free parameters. The filter in that study (Eastwood et al., 2015) was defined over the range from 1 Hz to 3 kHz. To obtain a broader range applicable to our simulation, i.e., from 0 Hz to 10 kHz, we used linear extrapolation.

## Results

As a first step toward determining how nematodes detect and respond to US stimulation, we placed single adult wild-type (N2) animals on sterile agar slabs and tracked their movement using a digital video camera and the Parallel Worm Tracker (Ramot et al., 2008) (Fig. 1). We subjected each animal to pulsed

ultrasound (10 MHz frequency, 200 ms duration, 1 kHz pulse repetition frequency at 50% duty) when it approached the US focus and found that this stimulus elicits robust reversal behavior (Fig. 2). Over 10 stimulus repetitions in 20 animals, a 1.0 MPa stimulus elicited rapid reversals and this response was not observed when a sham stimulus (0 MPa) was applied (Fig. 2A,B, Supplementary Movie 1,2).

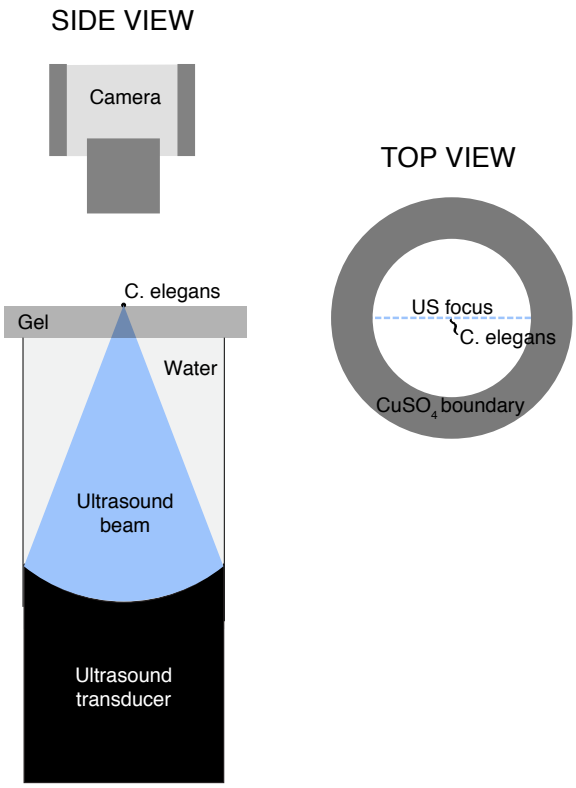


**Figure 1: Effects of ultrasound on neurons investigated using a behavioral-genetic assay in *C. elegans*.**

Side view. A single wild-type adult animal freely moves on an agar slab. A piezoelectric US transducer (10 MHz, 1-inch line-focused) on the bottom delivers an US stimuli. The interface between the face of the transducer and the agar slab is filled with degassed water. The animal's movement is tracked using a camera. Top view. The US transducer (10 MHz center frequency) had its beam focused on a line. We stimulated the animal when it approached the line of focus. The animal was maintained within the imaged scene using a copper sulfate boundary. Objects are not drawn to scale.

Behavioral responses were robust within and among all animals tested (Fig. 2B). We quantified whether in a given case a response to US was significant, i.e., whether an animal's change in direction due to US was statistically different from spontaneous changes in direction (reversals) known to occur

in isotropic conditions (Croll, 1975) and observed during our baseline measurements (see Materials and Methods for details). For each animal, we quantified the proportion of significant responses over the 10 stimulus repetitions, and refer to this metric as response frequency.

The response frequency increased with increasing US pressure applied (Fig. 2C). For the 0 MPa sham stimulus (Fig. 2A), the response frequency was indistinguishable from the spontaneous rate of responding (dotted line; $p = 0.52$, t-test, $n = 20$). The response significantly deviated from the baseline starting at 0.6 MPa ($p < 10^{-6}$). At 1 MPa (Fig. 2B) there was a significant response on average in 77.5% of trials. We fit the response-pressure curve with a sigmoid function and estimated that the half-activation pressure equals 0.71 MPa. A one-way ANOVA also detected a significant modulation of the response frequency by pressure ($F_{5,114} = 103.4$, $p < 10^{-39}$), reinforcing the idea that the probability of ultrasound-induced reversal depends on stimulus pressure.

We also tested the effect of the stimulus duration (Fig. 2D). In agreement with a previous study (Ibsen et al., 2015) responses were weak or absent when the stimulus was brief. Stimuli of 100 ms in duration or longer nonetheless produced substantial effects (Fig. 2D). There was a significant modulation of the response frequency by stimulus duration (one-way ANOVA, $F_{3,76} = 30.8$, $p < 10^{-12}$). The response frequency did not increase substantially beyond stimulus duration of 200 ms (response frequency at 200 ms versus 400 ms: $p = 0.24$, paired t-test, $n = 20$). Therefore, we used a stimulus duration of 200 ms for subsequent experiments.

A long-standing hypothesis has been that US delivers mechanical stimuli (loads) on neuronal tissues

---

**Figure 2 *(following page)*: Ultrasound elicits reversals in wild-type *C. elegans*.**

A) Raster plots showing each animal's heading as a function of time. The heading angle is encoded in color (see color bar) such that headings similar to the average angle in the 1 s window immediately preceding the US onset are shown in blue and reversals are encoded in yellow. A sham stimulus (0 MPa) was delivered at 0 s for 200 ms.
B) Raster plots of responses to 200 ms US pulses (delivered at 1.0 MPa).
In A and B, the diagrams on top are body contours of a representative response to a shame stimulus (A) or 1.0 MPa stimulus (B). In the raster plots shown in both panels, each row represents a single trial for a single animal and blocks correspond to ten trials delivered to each animal. A total of 20 animals were assayed, as described in Materials and Methods.
C) Effect of stimulus pressure. Points are mean±s.e.m. ($n = 20$) for animals stimulated at each of the six pressure values for a total of 10 trials. The smooth curve was fit to the data according to: $F = \frac{F_{max}}{1+\exp\left(\frac{P-P_{1/2}}{\text{slope}}\right)} + \text{base}$, where $F$ is the response frequency, $P$ is the pressure. The fit parameters were $F_{max} = 83\%$; $P_{1/2} = 0.71$ MPa, slope = 0.15, base = 5%.
D) Effect of stimulus duration. Same format as in C for the 1.0 MPa stimulus tested at different stimulus durations. The 200 ms datapoint was taken from C. In both C and D, the dotted line represents baseline rate of responding (see Materials and Methods). Smooth line is an exponential fit to the data with a time constant of 90 ms.

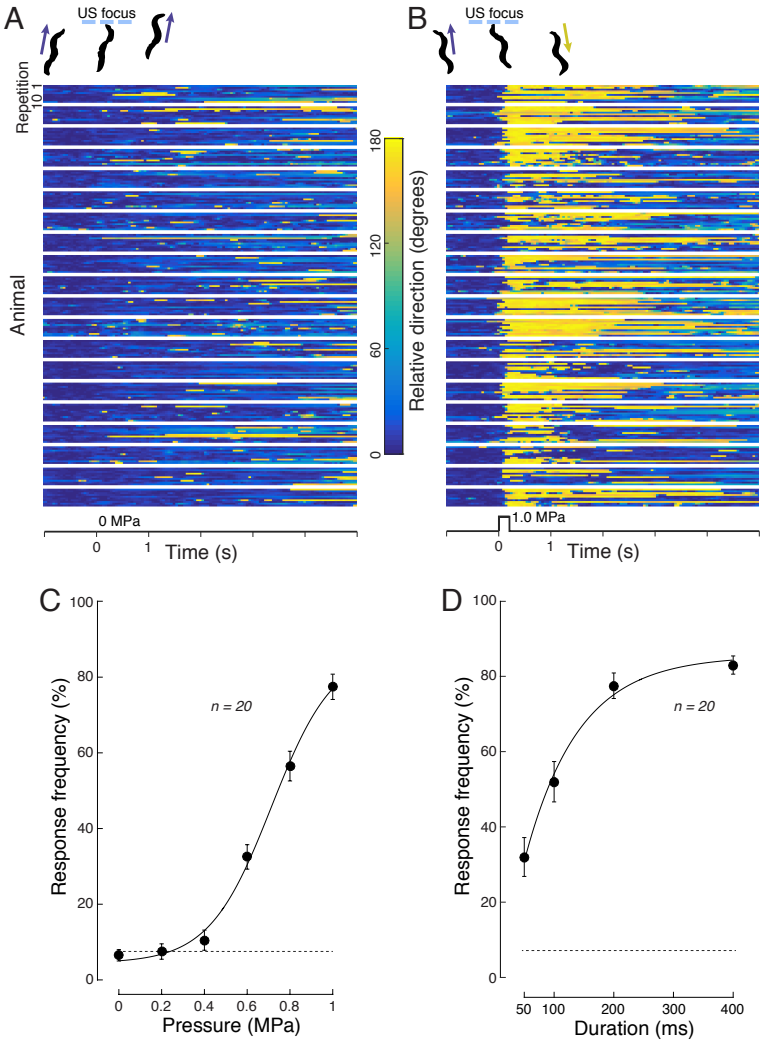

that are sufficient to activate neurons. A predominant alternative hypothesis has been that the effects on the nervous system reflect US-induced heating. We sought to exploit the response of wild-type worms to distinguish between these possibilities. To achieve this goal, we compared the responses to US in mutants deficient in thermosensation and mechanosensation.

First, we compared US-evoked behaviors in wild-type and *gcy-23(nj37)gcy-8(oy44)gcy-18(nj38)* mutants that lack the ability to sense tiny thermal fluctuations in temperature (Ramot et al., 2008; Wasserman et al., 2011). As shown in Fig. 3A, the response of the mutants was indistinguishable from that of wild type animals. We fit this curve to estimate the half-maximal pressure whose value was similar to that found for wild-type animals: $P_{1/2} = 0.71$ MPa and 0.76 MPa for wild-type and *gcy-23(nj37)gcy-8(oy44)gcy-18(nj38)* mutants, respectively. The mutants retained modulation by stimulus pressure, as assessed by one-way ANOVA ($F_{5,114} = 80.7$, $p < 10^{-35}$). Furthermore, as expected from the plot, a two-way ANOVA with factors animal strain and pressure failed to detect a significant difference between the strains ($F_{1,228} = 0.02$, $p = 0.89$) as well as the strain $\times$ pressure interaction ($F_{5,228} = 1.40$, $p = 0.23$). Thus, the ability to sense thermal fluctuations is not required for US-induced reversal behaviors. This finding suggests that US-induced heating, if any, is below the $\approx 0.05$°C detection threshold for *C. elegans* thermoreceptor neurons (Ramot et al., 2008; Clark et al., 2007).

Having established that thermosensation is dispensable US-evoked reversals, we compared responses in wild-type animals and mutants defective in mechanosensation. Specifically, we quantified the responses in *mec-3(e1338)* mutants in which three sets of neurons known to participate in gentle and harsh touch sensation (TRN, PVD, FLP) fail to differentiate properly (Way and Chalfie, 1989). The six touch receptor neurons (TRNs) are required for sensing gentle touch and the two pairs of multidendritic PVD and FLP neurons act as polymodal sensors of mechanical and nociceptive stimuli (Schafer, 2015). We found that *mec-3* mutants are insensitive to US stimulation (Fig. 3B) and moved at an average speed that was similar to wild type, measured 1 s period preceding the US onset (wildtype: 0.21 mm/s; *mec-3*: 0.17 mm/s; $p = 0.11$, $n = 20$, t-test). These values are within the range of values reported previously for wild-type animals (Ramot et al., 2008). Moreover, *mec-3* mutants showed no significant modulation of the response frequency by pressure ($F_{5,114} = 1.18$, $p = 0.32$, one-way ANOVA). Furthermore, as expected from the plot, the two-way ANOVA detected both a highly significant difference between the strains ($F_{1,228} = 246.1$, $p < 10^{-37}$) and a highly significant strain $\times$ pressure interaction ($F_{5,228} = 56.8$, $p < 10^{-37}$). This result shows that the *mec-3*-dependent mechanoreceptor neurons are required for US-evoked reversals and suggests that US can exert forces on neural tissue sufficient to activate these sensory neurons.

We next tested US-evoked behavior in *mec-4(e1611)* mutants that specifically lack the TRN neurons

(Driscoll and Chalfie, 1991), but retain PVD and FLP. As in *mec-3* mutants, US failed to evoked reversals in *mec-4(e1611)* (Fig. 3C) and there was no significant modulation of the response frequency by the US pressure amplitude in these animals (Fig. 3C; $F_{5,114} = 1.47$, $p = 0.20$). Moreover, a two-way ANOVA detected a highly significant difference between the strains and a highly significant strain $\times$ pressure interaction (both $p < 10^{-36}$). Thus, the TRN neurons, which can detect forces as small as 100 nN (O'Hagan et al., 2005), are required for behavioral responses to US stimulation in *C. elegans*.

Having identified the neurons involved in the response to the US, we next investigated which molecules within these neurons mediate the effect. Of particular interest, the TRN neurons express a sodium channel of the DEG/ENaC family that is required for sensing gentle touch stimuli (Suzuki et al., 2003; O'Hagan et al., 2005). The mechanosensitive function of DEG/ENaC ion channels in the TRN neurons critically depends on the expression of a pore-forming subunit (MEC-4), which is specific to these neurons. As in *mec-3* and *mec-4(e1611)* mutants, we found that *mec-4* null mutants are insensitive to US stimulation (Fig. 3D). These animals showed no significant modulation of the response frequency by the US pressure ($F_{5,114} = 0.37$, $p = 0.87$), and there was a highly significant difference between the wildtypes and the mechanomutants and a highly significant strain $\times$ pressure interaction (both $p < 10^{-35}$, two-way ANOVA). Although the responses in mechano-mutants seem to exhibit a trend to modulation by pressure (Fig. 3B-D), in no case was the modulation significant ($p > 0.09$, one-way ANOVA). Collectively, these results establish that behavioral responses to focused US depend on the TRNs and the MEC-4 protein which is an essential pore-forming subunit of the ion channel responsible for transducing touch in the TRNs.

Thus far, we have shown that focused US evokes reversal behaviors in freely moving *C. elegans* nematodes in a pressure- and stimulus duration-dependent manner (Fig. 2) and that such responses depend on the animal's ability to detect mechanical but not thermal stimuli (Fig. 4). These results suggest that US exerts its effect on excitable tissues *via* mechanical rather than thermal energy.

A previous study proposed that the responses to US in *C. elegans* are in part mediated by the TRP-4 ion channel (Ibsen et al., 2015). Using the same strain as the one used by Ibsen et al. (VC1141 *trp-4(ok1605)*), we also observed a modest deficit in US-evoked behavior (Fig. 5A). The two-way ANOVA detected both a significant main effect of strain ($F_{1,228} = 17.8$, $p < 0.0001$) and a significant strain $\times$ pressure interaction ($F_{5,228} = 4.8$, $p = 0.0003$). Thus, these mutants can detect US, but exhibit either a decreased sensitivity to US or a compromised ability to execute US-evoked behaviors.

To learn more about the nature of this deficit and because we also observed that these mutants grew slowly compared to wild-type animals, we tested two additional putative null allels of the *trp-4* gene: *gk341* and *sy695*. All three alleles, *ok1605*, *gk341*, and *sy695* are expected to encode deletions in the

*trp-4* gene, which we verified by PCR analysis of genomic DNA (see Methods for details). Despite the expectation that all three *trp-4* deletion alleles would have the same US phenotype, we found that *gk341* and *sy695* mutants responded to US just like wild-type animals (Fig. 5B; two-way ANOVAs, main effects and interactions $p > 0.29$). These findings suggested that the deficit in the VC1141 *trp-4(ok1605)* animals might be due to a mutation present in the genetic background. To test this, we out-crossed the *trp-4(ok1605)* animals with wild-type animals four times while tracking the *trp-4* mutation *via* PCR. The resulting animals, GN716 *trp-4(ok1605)*, had US-evoked behaviors that were indistinguishable from wild-type (Fig. 5B; two-way ANOVA, main effect and interaction $p > 0.23$). These results are summarized for the pressure of 1 MPa in Fig. 5C and suggest that the defect in responses of the *trp-4(ok1605)* animals is due to mutation/s in the genetic background of this strain. Additional work will be needed to determine the nature of the mutations responsible for the apparent decrease in US sensitivity.

The finding that mechanosensation is essential for US effects suggests a strategy for optimizing US parameters to achieve most effective stimulation. In particular, we repeated our 200 ms stimulus and varied pulse repetition frequencies (PRFs) in the range from 30 Hz to 10 kHz, while keeping duty cycle at 50%. US indeed evoked reversals in a frequency-dependent manner (Fig. 6A). Responses were maximal in the range of 300–1000 Hz, and diminished in both directions away from that optimal frequency range. The shape of the curve follows the prediction (Fig. 6A, green) derived from a model linking tissue mechanics to MEC-4-dependent channel activation (Eastwood et al., 2015). We note that since stimuli were delivered at 50% duty cycle at all the tested frequencies, the same amount of energy was delivered into the tissue at all pulse repetition frequencies. If the behavioral responses were the result of tissue heating, little or no modulation by the PRF would be expected. Yet, the plot shows and an ANOVA confirms a strong modulation of the response by the PRF ($F_{5,114} = 10.8$, $p < 10^{-7}$). This result corroborates the inference from our genetic dissection that mechanical effects of US account for neural stimulation.

We further hypothesized that discrete pulses—which provide repeated mechanical stimulation, should be more potent than continuous US stimuli. To test this idea, we compared the 1 kHz pulse repetition frequency, which delivers a 200 ms burst of 0.5 ms intervals stimulus On interval interleaved with 0.5 ms of stimulus Off (i.e. 50 % duty cycle) with a continuous (100% duty) 200 ms stimulus. For completeness, we also tested the values of 5, 10, 25, and 75% duty. Fig. 6B shows that the 50% duty cycle was more than three-times as potent in eliciting a response compared to the continuous (100% duty) protocol (77.5% compared to 24.0%, $p < 10^{-12}$, t-test). This is even though the continuous stimulation delivers twice as much energy into the tissue as the pulsed protocol of 50% duty. Interestingly, pulsed stimulation was found to be more effective than continuous stimulation in eliciting motor responses also in rats (Kim et al., 2014). Furthermore, as found here in *C. elegans*, 50% duty proved to be an optimal value in rats

(Kim et al., 2014). In addition, the response to changes in duty cycle indicates that the width of the individual mechanical events associated with the US can be quite brief—just 50 $\mu$s (5% of duty)—and still trigger appreciable behavioral responses (response rate of 34.0%, significantly different from baseline at $p < 0.0001$, t-test, $n = 20$). This is even though the energy delivered into the tissue is only 1/10th of that delivered at 50% duty. We captured the duty cycle response profile in Fig. 6B using a simple model that passes the ultrasound input through the frequency-dependent mechanotransduction system characterized in Fig. 6A (see Methods for details). There was a very tight correspondence between the data and the model's predictions ($r = 0.987$; Pearson's correlation for the individual data points shown in Fig. 6A), even though the model has no free parameters. These findings provide further support for the idea that US affects neurons *via* delivering mechanical energy.

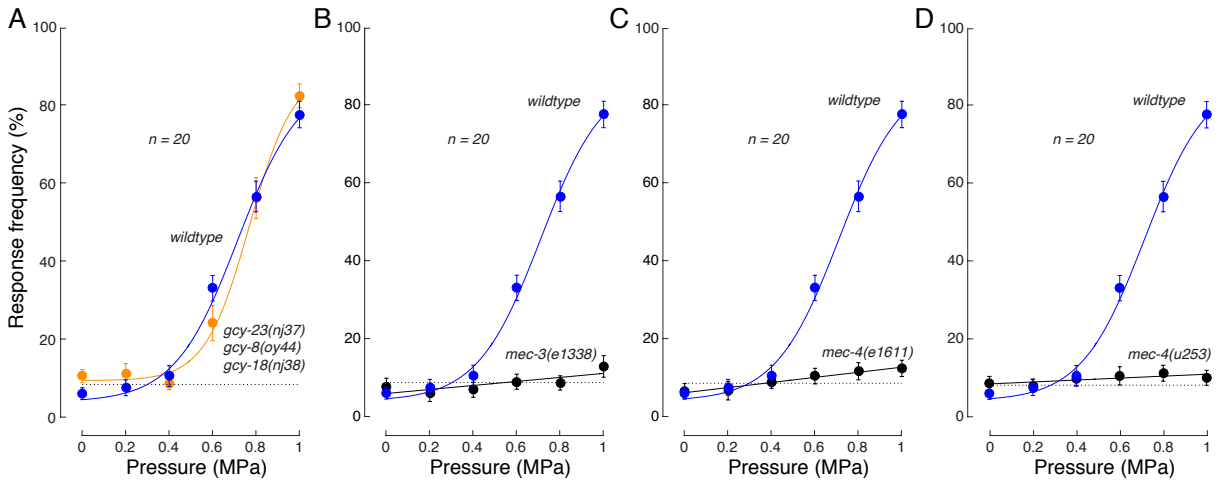


**Figure 3: The response to ultrasound is of mechanical nature.**
The effect of US in wildtype (blue curve in all panels, same data as in Fig. 2C) compared to effects in animals deficient in thermosensation (A) or mechanosensation (B, C, D).
A) Thermosensory mutant: *gcy-23(nj37)gcy-8(oy44)gcy-18(nj38)* triple mutant incapable of detecting changes in temperature. The curve represents fit with the sigmoid function. The data and fit for wild-types are the same as in Fig. 2C. Fitting parameters for *gcy-23(nj37)gcy-8(oy44)gcy-18(nj38)* are ($F_{max}$, $P_{1/2}$, slope, base): 80%, 0.76 MPa, 0.10, 9%.
B) Mechanosensory mutant (*mec-3(e1338)*) in which TRN, PVD, and FLP neurons are not properly differentiated.
C) Mechanosensory mutant (*mec-4(e1611)*) with degenerated TRN neurons.
D) Mechanosensory mutant (*mec-4(u253)*) lacking an essential pore-forming subunit (MEC-4) of the DEG/ENaC ion channel activated by touch.
Dotted line represents the average baseline response rate (see Materials and Methods) for each pair. There was no significant difference in baseline rates across the animal strains (see Methods).

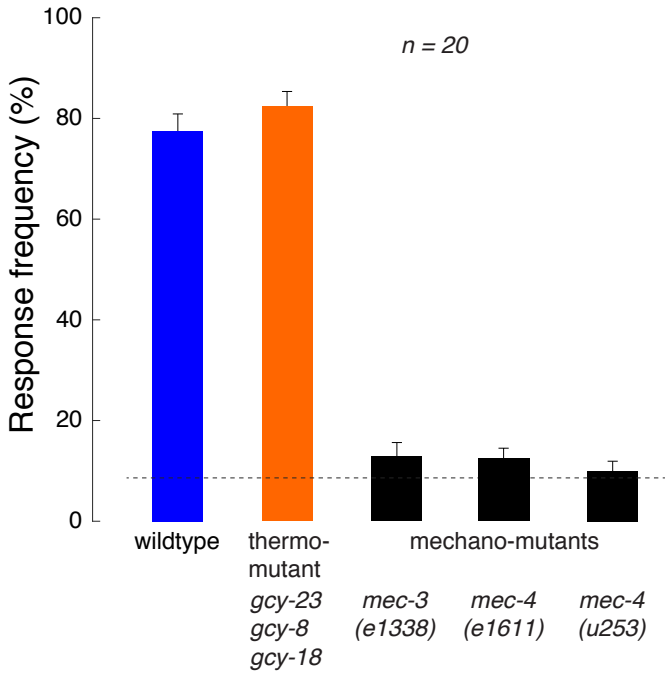


**Figure 4: Summary of the ultrasound effect on the individual strains.**

Data from Fig. 3 quantified at the pressure of 1 MPa. The dotted line represents the baseline response frequency averaged across the strains.

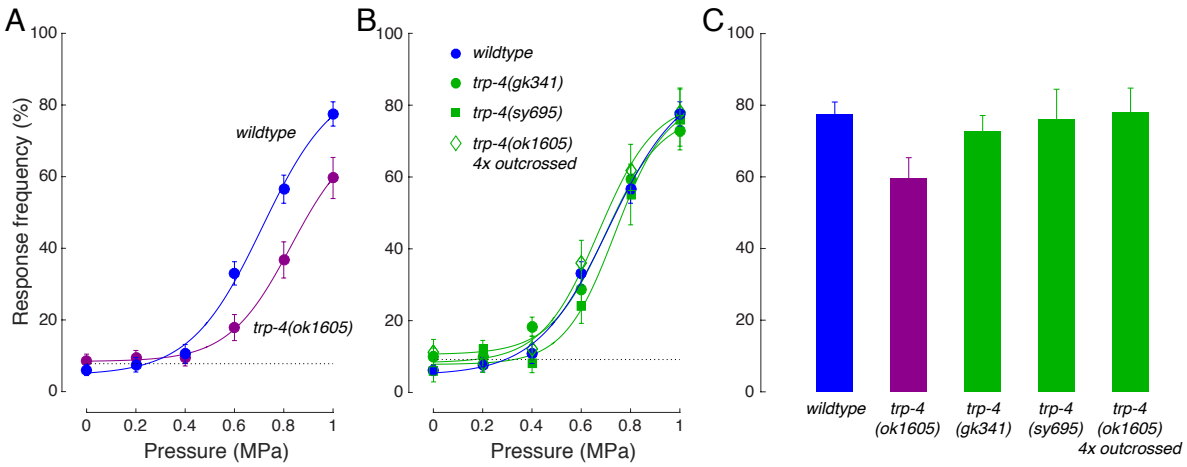


**Figure 5: Responses of *trp-4* mutants.**

A) *trp-4(ok1605)* mutants used in a previous study (Ibsen et al., 2015) contrasted with the wildtypes (data from Fig. 2C). The sigmoid fit to the *trp-4(ok1605)* data yielded $F_{max} = 65\%$; $P_{1/2} = 0.83$ MPa, slope = 0.13, base = 8%.

B) *trp-4(gk341)* mutants, *trp-4(sy695)* mutants, and *trp-4(ok1605)* mutants outcrossed four times with wildtypes (N2).

C) Summary of the *trp-4* analysis quantified at 1 MPa.

Dotted line represents the average baseline response rate (see Materials and Methods) for each pair. We collected responses from $n = 20$ *wildtype*, *trp-4(ok1605)*, and *trp-4(gk341)* animals and $n = 10$ from *trp-4(sy695)* and *trp-4(ok1605) outcrossed* animals.

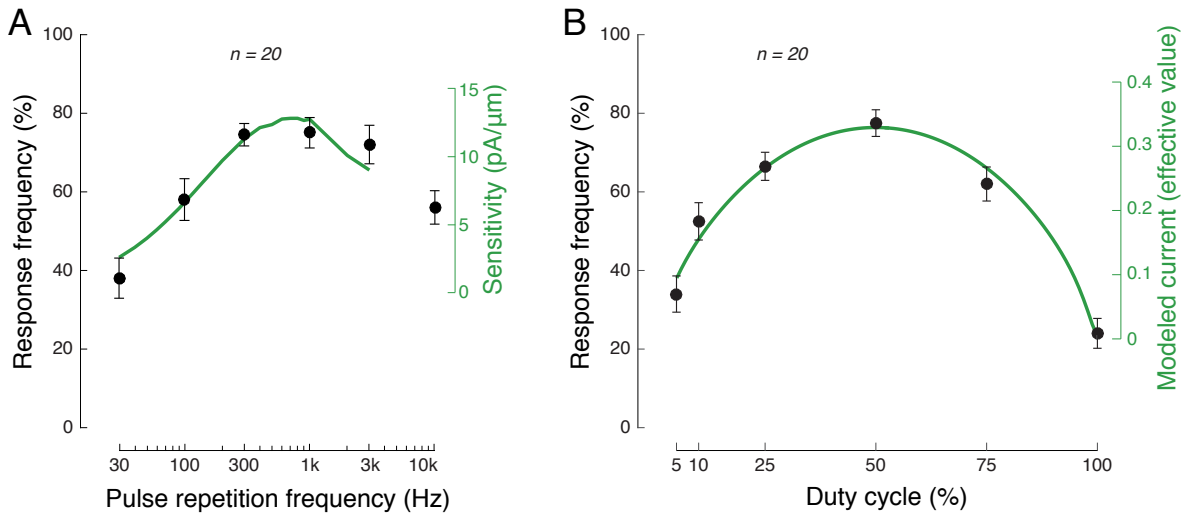


**Figure 6: Application of the findings of mechanical effects of ultrasound on neurons in optimizing stimulus parameters.**

A) Mean±s.e.m. response frequency of wildtype animals as a function of pulse repetition frequency. The duty cycle is 50% in all cases; therefore, all stimuli deliver the same amount of energy into the tissue. The curve superimposes modeled sensitivity of TRN currents in response to mechanical displacements occurring at specific pulse repetition frequencies (Eastwood et al., 2015).

B) Mean±s.e.m. response frequency of wildtype animals as a function of the duty cycle. The pulse repetition rate was 1 kHz, so a duty cycle of 5, 10, 25, 50, 75, 100% corresponds to a pulse width of 50 $\mu$s, 100 $\mu$s, 250 $\mu$s, 500 $\mu$s, 750 $\mu$s, and 1 ms (continuous wave, no off epochs), respectively. The curve superimposes modeled values of currents flowing through TRNs in response to stimuli of the respective duty cycle (see Methods for details). In both A and B, the pressure amplitude was 1 MPa, carrier frequency 10 MHz, and stimulus duration 200 ms.

# Discussion

How US stimulates neurons has been a mystery since the discovery of its neuromodulatory effects in 1929 (Harvey, 1929). Answers to this question have been vigorously sought, especially in recent years which have seen reports of US neuromodulatory effects in humans (Legon et al., 2014; Lee et al., 2015; Lee et al., 2016). To provide insights into the phenomenon, we developed a genetic dissection assay based on *C. elegans* nematodes. We found that focused ultrasound in the range of pressures previously used for neuromodulation elicits robust reversal behavior of the animals. The response was maintained in animals that are deficient in sensing tiny changes in temperature but was greatly reduced in animals that lack neurons that participate in mechanosensation. This suggests a mechanical nature of the effect.

It has been proposed that US may activate neurons by exerting mechanical forces on cellular membranes and thus activate mechanosensitive ion channels (Tyler et al., 2008; Tyler, 2012). On this front, we identified an ionotropic mechanosensor, MEC-4, that is required for US-evoked behaviors. In particular, the response was markedly reduced in mutants missing a pore-forming subunit of the DEG/ENaC ion channel. The DEG/ENaC ion channel consisting of the MEC-4 subunit is expressed in touch receptor neurons and is critically involved in the animal's sense of gentle touch. Animals that lack MEC-4 do not reverse direction when presented with traditional mechanical stimuli such as a mechanical probe applied to the head (Chalfie and Sulston, 1981) and lack touch-evoked mechanoreceptor currents (O'Hagan et al., 2005). This finding supports the hypothesis that the mechanical forces associated with US are of sufficient magnitude to act on mechanosensitive ion channels. Additional experiments are needed to determine whether US acts directly on the MEC-4-dependent channels or whether it acts on the membrane or intra/extra-cellular structures that support their function.

The findings that behavioral responses to US require mechanosensitive neurons and ion channels suggest that the response has a strong mechanical component. In this respect, there are two major phenomena associated with a propagating US wave. First, the target tissue, such as a cell membrane, experiences oscillations with period equal to the ultrasound carrier frequency. The pressures used for neuromodulation can cause appreciable particle displacement (on the order of 0.01–0.1 $\mu$m (Gavrilov et al., 1976)). Nonetheless, the displacement is distributed in sinusoidal fashion along the wavelength (about 100 $\mu$m at 10 MHz) of the propagating wave. This creates a very small displacement gradient (e.g., 0.1 $\mu$m per 100 $\mu$m). It is questionable whether such a small gradient can cause significant enough deformation of a pore segment of an ion channel with regard to the channel dimensions. Moreover, the primary pressure oscillations, which occur at the carrier frequency, cannot explain the frequency dependence of the responses (Fig. 6A). The second candidate is acoustic radiation force. The radiation force is a non-linear phenomenon associated with momentum transfer from the US wave field to the

medium (Duck et al., 1998). Acoustic radiation force exerts a steady pressure on a target throughout the time of US application. This steady pressure may stretch a cell membrane to an extent that affects conformation states of ion channels embedded within the membrane. The acoustic radiation force may also induce acoustic streaming of the fluid near a neuron, which may further contribute to shear stress on the cell membrane (Tyler, 2011).

The investigation of optimal stimulus parameters (Fig. 6) has relevance to ultrasound neuromodulation in mammals. In particular, the optimal value of 50% duty (Fig. 6B) has also been found to be optimal in rats (Kim et al., 2014). Furthermore, the optimal range of pulse repetition frequencies identified here (300–1000 Hz) mirrors the range used in higher mammals (Deffieux et al., 2013; Legon et al., 2014; Lee et al., 2015; Lee et al., 2016; Lee et al., 2016). In this regard, our data and the model of Eastwood et al. (Eastwood et al., 2015) provide specific insights into the frequency dependence of the neurostimulatory effects. In particular, the Eastwood et al. model provides predictions that are quite general, only assuming that ion channels that sense mechanical stimuli are anchored through a filament to a viscous extracellular or intracellular matrix. Such an architecture can exist in other organisms and nervous system structures, including Pacinian corpuscules in mammals (Eastwood et al., 2015). Furthermore, the finding that mechano-electrical transduction of biological tissues can show a substantial dependence on the frequency of impending mechanical pulses (Fig. 6A) can be used to understand and optimize neuromodulatory effects of specific stimulus parameters. For instance, this frequency dependence can be used, by itself, to capture the effect of stimulus duty cycle (Fig. 6B). This approach is applicable to interpreting and optimizing effects associated with particular stimulus parameters in any biological tissue that exhibits mechano-electrical transduction properties (Kim et al., 2014).

A previous study suggested that US triggers reversal behavior in *C. elegans* only when US-effect-enhancing microbubbles are added to the agar substrate (Ibsen et al., 2015). We tested a wide range of US parameters and found that short (Fig. 2D) and continuous (Fig. 6A) stimuli, similar to those used previously (a continuous stimulus 10 ms in duration), indeed produce weak responses. Nonetheless, we found that when the US is delivered in pulses (e.g., 50% duty in Fig. 6A) of sufficient duration (Fig. 2D), it elicits robust reversal responses in wild-type animals. Such responses depend on mechanoreceptor neurons and an ionotropic mechanosensory receptor. The picture emerging from the present work and a previous one (Kubanek et al., 2016) is that US can activate mechanosensitive ion channels without the use of microbubbles.

Besides applications in neuromodulation, the finding of a mechanosensitive nature of the effect of US on neurons has implications for basic studies of mechanosensation. Specifically, US can be pulsed at a very high frequency (up to thousands of kHz) and with very high temporal precision (several microseconds

of propagation time). Data such as those provided in Fig. 6A can now be used to validate models of mechanosensation (Eastwood et al., 2015).

In summary, this work suggests that behavioral responses to US rest on neurons and ion channels that are critical in sensing mechanical stimuli. Because many neurons and ion channels in the brain and in the periphery posses mechanosensitive properties, the findings of this study highlight one of the mechanisms using which US can activate neurons. The mechanical essence of the effect identified here suggests specific ways to optimize the stimulation parameters. This paves the way to applying US as a new tool to study the function of neural circuits and to applying US as a spatially precise clinical tool to alleviate neurological disorders.

## Acknowledgements

We thank our Stanford colleagues, Z. Liao, M. Menz, P. Ye, M. Prieto for laboratory and technical assistance and input on the experimental design; and M. Maduke, P. Khuri-Yakub, K. Butts-Pauly, M. Menz, M. Prieto, and J. Brown for helpful comments. We also thank Z. Pincus (Washington University, St. Louis) for providing animals for an initial experiments. This work was supported by grants from NIH (R01NS047715, R01NS092099), gifts from the Stanford Neuroscience Institute and Mathers Foundation (to MBG, SB) and a Stanford Medicine Dean's fellowship (to JK).

## Author contributions

J.K., S.B., and M.B.G. developed the concept; J.K. and P.S. collected behavioral data; A.D. prepared and validated the *trp-4* strains; J.K. analyzed the data; and J.K., S.B., M.B.G. wrote the paper.

## References

Chalfie M, Sulston J (1981) Developmental genetics of the mechanosensory neurons of caenorhabditis elegans. *Developmental biology* 82:358–370.

Clark DA, Gabel CV, Gabel H, Samuel AD (2007) Temporal activity patterns in thermosensory neurons of freely moving caenorhabditis elegans encode spatial thermal gradients. *The Journal of neuroscience* 27:6083–6090.

Croll NA (1975) Components and patterns in the behaviour of the nematode caenorhabditis elegans. *Journal of zoology* 176:159–176.

Deffieux T, Younan Y, Wattiez N, Tanter M, Pouget P, Aubry JF (2013) Low-intensity focused ultrasound modulates monkey visuomotor behavior. *Current Biology* 23:2430–2433.

Driscoll M, Chalfie M (1991) The mec-4 gene is a member of a family of caenorhabditis elegans genes that can mutate to induce neuronal degeneration .

Duck FA, Baker AC, Starritt HC (1998) *Ultrasound in medicine* CRC Press.

Eastwood AL, Sanzeni A, Petzold BC, Park SJ, Vergassola M, Pruitt BL, Goodman MB (2015) Tissue mechanics govern the rapidly adapting and symmetrical response to touch. *Proceedings of the National Academy of Sciences* 112:E6955–E6963.

Foster KR, Wiederhold ML (1978) Auditory responses in cats produced by pulsed ultrasound. *The Journal of the Acoustical Society of America* 63:1199–1205.

Fry F et al. (1958) Production of reversible changes in the central nervous system by ultrasound. *Science* 127:83–84.

Garrity PA, Goodman MB, Samuel AD, Sengupta P (2010) Running hot and cold: behavioral strategies, neural circuits, and the molecular machinery for thermotaxis in c. elegans and drosophila. *Genes & development* 24:2365–2382.

Gavrilov L, Gersuni G, Ilyinsky O, Sirotyuk M, Tsirulnikov E, Shchekanov E (1976) The effect of focused ultrasound on the skin and deep nerve structures of man and animal. *Progress in brain research* 43:279–292.

Gavrilov L, Tsirulnikov E, Davies IaI (1996) Application of focused ultrasound for the stimulation of neural structures. *Ultrasound in medicine & biology* 22:179–192.

Glauser DA, Goodman MB (2016) Molecules empowering animals to sense and respond to temperature in changing environments. *Current Opinion in Neurobiology* 41:92–98.

Harvey EN (1929) The effect of high frequency sound waves on heart muscle and other irritable tissues. *American Journal of Physiology–Legacy Content* 91:284–290.

Ibsen S, Tong A, Schutt C, Esener S, Chalasani SH (2015) Sonogenetics is a non-invasive approach to activating neurons in caenorhabditis elegans. *Nature communications* 6.

Kim H, Chiu A, Lee SD, Fischer K, Yoo SS (2014) Focused ultrasound-mediated non-invasive brain stimulation: examination of sonication parameters. *Brain stimulation* 7:748–756.

King RL, Brown JR, Newsome WT, Pauly KB (2013) Effective parameters for ultrasound-induced in vivo neurostimulation. *Ultrasound in medicine & biology* 39:312–331.

Krasovitski B, Frenkel V, Shoham S, Kimmel E (2011) Intramembrane cavitation as a unifying mechanism for ultrasound-induced bioeffects. *Proceedings of the National Academy of Sciences* 108:3258–3263.

Kubanek J, Shi J, Marsh J, Chen D, Deng C, Cui J (2016) Ultrasound modulates ion channel currents. *Scientific reports* 6.

Lee W, Kim HC, Jung Y, Chung YA, Song IU, Lee JH, Yoo SS (2016) Transcranial focused ultrasound stimulation of human primary visual cortex. *Scientific Reports* 6:34026.

Lee W, Kim H, Jung Y, Song IU, Chung YA, Yoo SS (2015) Image-guided transcranial focused ultrasound stimulates human primary somatosensory cortex. *Scientific reports* 5.

Lee W, Lee SD, Park MY, Foley L, Purcell-Estabrook E, Kim H, Fischer K, Maeng LS, Yoo SS (2016) Image-guided focused ultrasound-mediated regional brain stimulation in sheep. *Ultrasound in medicine & biology* 42:459–470.

Legon W, Sato TF, Opitz A, Mueller J, Barbour A, Williams A, Tyler WJ (2014) Transcranial focused ultrasound modulates the activity of primary somatosensory cortex in humans. *Nature Neuroscience* 17:322–329.

Menz MD, Oralkan Ö, Khuri-Yakub PT, Baccus SA (2013) Precise neural stimulation in the retina using focused ultrasound. *The Journal of Neuroscience* 33:4550–4560.

Meyers R, Fry WJ, Fry FJ, Dreyer LL, Schultz DF, Noyes RF (1959) Early experiences with ultrasonic irradiation of the pallidofugal and nigral complexes in hyperkinetic and hypertonic disorders. *Journal of neurosurgery* 16:32–54.

O'Hagan R, Chalfie M, Goodman MB (2005) The mec-4 deg/enac channel of caenorhabditis elegans touch receptor neurons transduces mechanical signals. *Nature neuroscience* 8:43–50.

Plaksin M, Shoham S, Kimmel E (2014) Intramembrane cavitation as a predictive bio-piezoelectric mechanism for ultrasonic brain stimulation. *Physical Review X* 4:011004.

Prieto ML, Oralkan Ö, Khuri-Yakub BT, Maduke MC, Phillips W (2013) Dynamic response of model lipid membranes to ultrasonic radiation force. *PloS one* 8.

414 Ramot D, Johnson BE, Berry Jr TL, Carnell L, Goodman MB (2008) The parallel worm tracker: a
415 platform for measuring average speed and drug-induced paralysis in nematodes. *PloS one* 3:e2208.

416 Ramot D, MacInnis BL, Goodman MB (2008) Bidirectional temperature-sensing by a single
417 thermosensory neuron in c. elegans. *Nature neuroscience* 11:908–915.

418 Rohr KR, Rooney J (1978) Effect of ultrasound on a bilayer lipid membrane. *Biophysical journal* 23:33.

419 Schafer WR (2015) Mechanosensory molecules and circuits in c. elegans. *Pflügers Archiv-European*
420 *Journal of Physiology* 467:39–48.

421 Stiernagle T (2006) Maintenance of c. elegans (february 11, 2006), wormbook, ed. the c. elegans research
422 community, wormbook, doi/10.1895/wormbook. 1.101. 1.

423 Suzuki H, Kerr R, Bianchi L, Frøkjær-Jensen C, Slone D, Xue J, Gerstbrein B, Driscoll M, Schafer WR
424 (2003) In vivo imaging of c. elegans mechanosensory neurons demonstrates a specific role for the mec-4
425 channel in the process of gentle touch sensation. *Neuron* 39:1005–1017.

426 Tufail Y, Matyushov A, Baldwin N, Tauchmann ML, Georges J, Yoshihiro A, Tillery SIH, Tyler WJ
427 (2010) Transcranial pulsed ultrasound stimulates intact brain circuits. *Neuron* 66:681–694.

428 Tufail Y, Yoshihiro A, Pati S, Li MM, Tyler WJ (2011) Ultrasonic neuromodulation by brain stimulation
429 with transcranial ultrasound. *Nature Protocols* 6:1453–1470.

430 Tyler WJ (2011) Noninvasive neuromodulation with ultrasound? a continuum mechanics hypothesis.
431 *The Neuroscientist* 17:25–36.

432 Tyler WJ (2012) The mechanobiology of brain function. *Nature Reviews Neuroscience* 13:867–878.

433 Tyler WJ, Tufail Y, Finsterwald M, Tauchmann ML, Olson EJ, Majestic C (2008) Remote excitation
434 of neuronal circuits using low-intensity, low-frequency ultrasound. *PLoS One* 3:e3511.

435 Wasserman SM, Beverly M, Bell HW, Sengupta P (2011) Regulation of response properties and operating
436 range of the afd thermosensory neurons by cgmp signaling. *Current Biology* 21:353–362.

437 Way JC, Chalfie M (1989) The mec-3 gene of caenorhabditis elegans requires its own product for
438 maintained expression and is expressed in three neuronal cell types. *Genes & development* 3:1823–1833.

439 Yoo SS, Bystritsky A, Lee JH, Zhang Y, Fischer K, Min BK, McDannold NJ, Pascual-Leone A, Jolesz
440 FA (2011) Focused ultrasound modulates region-specific brain activity. *Neuroimage* 56:1267–1275.